from 1 to 9 kHz although the effect was greater at frequencies higher than 1 kHz.

Although the compliance of the tendons could influence the stiffness measured on the tetanus rise, especially in this very short preparation, we find it unlikely that tendon compliance could account for our data (*7*). The lead of stiffness over force during the tetanus rise can be explained by assuming there is a relatively long-lived crossbridge state between attachment and force generation. Such a state was proposed by H. E. Huxley (*8*) on the basis of the observation that the equatorial x-ray diffraction pattern from contracting frog muscle changes more rapidly than force during the tetanus rise.

To summarize, the fall in force after a step release is accompanied by a much smaller fall in stiffness. Most of this fall in stiffness is due to tendon compliance. This is consistent with observations reported by others (*5*, *6*). However, the fact that stiffness increased more rapidly than force during the tetanus rise suggests that crossbridge attachment might be followed by a significant delay before force develops.

GIOVANNI CECCHI
PETER J. GRIFFITHS
STUART TAYLOR*

Department of Pharmacology,
Mayo Foundation,
Rochester, Minnesota 55905

References and Notes

1. A. F. Huxley and R. M. Simmons, *Nature (London)* **233**, 533 (1971).
2. L. E. Ford, A. F. Huxley, R. M. Simmons, *J. Physiol. (London)* **311**, 219 (1981).
3. ———, *ibid.* **269**, 441 (1977).
4. Isolated single muscle fibers were dissected from lumbricalis" digiti IV muscles of *Rana temporaria*. Aluminum clips were attached to the tendons at each end to reduce tendon compliance. The fibers were then transferred to a small chamber and suspended between a length step generator (*9*) and a force transducer (*10*). The amount of compliance in a preparation was estimated by performing rapid step length changes and plotting the force at the end of the step against the step amplitude to obtain T_1 curves (*1*). The amount of instantaneous shortening sufficient to just discharge isometric force (y_0) was determined by extrapolating the linear portion of the T_1 curve (for instance, Fig. 1). In some experiments on single fibers from tibialis anterior muscles, the stiffness measured by sinusoidal length changes had higher apparent values than expected and there was a considerable phase lag of force relative to length. Thus fibers behaved like a uniform elastic rod in which a natural mode of vibration was excited by length oscillations. Since tibialis anterior fibers were longer than those from lumbricalis" digiti IV muscles (5.6 to 7.3 mm compared to 1.5 to 2.6 mm), their resonance frequency was lower. The resonance frequency of the fiber used for Fig. 1, estimated from the transmission time, was about 40 kHz during the tetanus plateau. This is in good agreement with the theoretical value obtained by assuming a fiber behaves as a uniform elastic rod and viscous forces are negligible [M. Schoenberg, J. B. Wells, R. J. Podolsky, *J. Gen. Physiol.* **64**, 623 (1974)].
5. L. E. Ford, A. F. Huxley, R. M. Simmons, *J. Physiol. (London)* **240**, 42P (1974).
6. F. J. Julian and D. L. Morgan, *ibid.* **319**, 193 (1981).
7. (i) A different interpretation is possible if we assume that our data may be influenced by the elastic properties of the tendons. If there were a constant ratio of stiffness to force during the tetanus rise, and if the amount of instantaneous shortening necessary to just discharge the force developed by the crossbridges was assumed to be constant at about 4 nm per half-sarcomere (*3*), it should be possible to estimate tendon compliance on the tetanus rise and on the plateau from the observed value of y_0. Such measurements imply that there was higher tendon stiffness on the rise than at the plateau, which is unlikely. Our results could also be explained by assuming that a large portion of the fiber compliance resides in the filaments and the Z line. However, the compliance of the filaments and Z line is likely to be only about 10 percent of the total fiber compliance (*2*); this is too small to account for our results. (ii) Another alternative is that the low level of fiber stiffness during the tetanus rise reduced the resonance frequency of the fiber, causing significant amplification of the force oscillations. This may have some basis at very low levels of stiffness. However, the relative stiffnesses at 4 and 7 kHz during the tetanus rise were not significantly different and did not show detectable phase shift. Furthermore, calculations on the assumption that a fiber behaved as an undamped elastic rod—the worst possible case—indicated that such an effect is not large enough to account for the observed deviation from a constant ratio of stiffness to force. (iii) The presence of some degree of shortening against tendon compliance could be another explanation for our findings. According to previous data [A. F. Huxley and R. M. Simmons, *Cold Spring Harbor Symp. Quant. Biol.* **37**, 669 (1973); F. J. Julian and M. R. Sollins, *J. Gen. Physiol.* **66**, 287 (1975)] and the model of A. F. Huxley [*Prog. Biophys. Biophys. Chem.* **7**, 255 (1957)], shortening would tend to increase the ratio of stiffness to force. However, a rough calculation shows that an improbably large amount of shortening at the expense of tendons would have to occur during the tetanus rise. The first point on the tetanus rise in Fig. 2, which was measured with 4-kHz oscillations, has a ratio of 1.9. According to the Huxley model, such a ratio is only attained at a shortening velocity of 2.2 mm/sec (0.37 times the maximum velocity, V_{max}). At the second point measured with 4 kHz the ratio is consistent with a velocity of 1.8 mm/sec (0.30 V_{max}). The time elapsed between these measurements was 4.5 msec. Taking the worst case—the slowest velocity—as the average shortening velocity during this period, then the tendons should have been extended by 8.1 μm as force increased from 0.22 to $0.27P_0$. However, the T_1 curve for this fiber indicates that the extension of the total fiber compliance from 0.22 to $0.27P_0$ was less than 1.8 μm. Consequently, such a degree of tendon extension seems impossible.
8. H. E. Huxley, *Cross-Bridge Mechanism in Muscle Contraction*, H. Sugi and G. H. Pollack, Eds. (Univ. of Tokyo Press, Tokyo, 1979), pp. 391–405.
9. G. Cecchi, F. Colomo, V. Lombardi, *Boll. Soc. Ital. Biol. Sper.* **52**, 733 (1976).
10. A. F. Huxley and V. Lombardi, *J. Physiol. (London)* **305**, 15P (1980).
11. We are indebted to L. F. Wussow for preparing the figures and the manuscript, to L. A. Wanek for technical assistance, to R. Rüdel for helpful criticism, and to the Minnesota Heart Association, Muscular Dystrophy Association, and U.S. Public Health Service (grant NS 14268) for support.
* Address correspondence to S.T.

24 December 1981; revised 5 April 1982

Loss of Retinal X-Cells in Cats with Neonatal or Adult Visual Cortex Damage

Abstract. *Recordings were made from single retinal ganglion cell somas in cats whose visual cortical areas 17 and 18 were damaged on the day of birth or in adulthood. Neonatal lesions produced a 78 percent loss of X-cells in the retina, while lesions made in adulthood produced a 22 percent loss. Y-cells and W-cells were unaffected. This retinal abnormality needs to be considered when interpreting studies of behavioral deficits and neural mechanisms of recovery after damage to the visual cortex.*

Damage to visual cortical areas of the brain in adult mammals (including humans) results in severe deficits in visual abilities, although some behavioral recovery does occur (*1*). If similar brain damage is incurred neonatally, the resultant behavioral disabilities can be much less severe; indeed, the animals can perform normally on many tasks when mature (*1*). In correspondence with these behavioral results, anatomical and physiological studies indicate that anomalous neural connections can develop in the central visual pathways after neonatal, but not adult, brain damage (*2*). This suggests that functional compensation by the central nervous system may underlie the superior recovery of behavior after neonatal lesions. But to fully understand the neural basis of both the initial deficits and the subsequent recovery, it is necessary to know the nature of the inputs to the system.

Anatomical studies indicate that the retina is abnormal after visual cortical damage. Marked transneuronal retrograde degeneration of retinal ganglion cells follows cortical lesions in neonatal cats and monkeys, and less severe degeneration follows lesions in adult monkeys and humans (*3–7*). Analysis of soma sizes and central projections of the remaining ganglion cells in the affected retinas led to the suggestion that the degenerated ganglion cells are primarily of the X-cell (*8*) functional class (*4*, *5*, *7*). However, the physiological properties of the retina after visual cortical damage have never, to our knowledge, been studied in any species. We therefore sought to determine the functional properties of retinal ganglion cells in adult cats given visual cortical lesions as neonates or as adults. We found that W- and Y-type ganglion cells are present in normal numbers and have normal response properties. However, a marked loss of X-type ganglion cells follows neonatal lesions and a smaller loss follows adult damage.

0036-8075/82/0702-0072$01.00/0

Three groups of cats were studied: six normal adults, seven adults given visual cortical lesions as neonates, and five cats with adult lesions. All lesions were unilateral and were made by aspiration after removal of the overlying bone and retraction of the meninges. The lesions were intended to remove the lateral and postlateral gyri, which include areas 17, 18, and part of 19 (*9*). The neonatal lesions were made within 24 hours of birth, and retinal recordings were carried out 8.5 to 14.5 months later. Cats with adult lesions were studied 10 to 15 months after surgery. There was no significant correlation between survival time and the results obtained for either group.

Ganglion cell soma recordings were made from the retinal surface with intraocular micropipettes in paralyzed cats anesthetized with 70 percent N_2O and 30 percent O_2 (*10*). The recordings were made from the nasal retina (5° to 15° from area centralis) of the eye contralateral to the lesion, that is, from a region that normally projects exclusively to the hemisphere with the lesion. We used a standardized sampling procedure (*10*) to compare estimates of the density of ganglion cell soma recordings as well as the relative proportions of X-, Y-, and W-cells encountered in each group of cats.

Visual stimuli were presented on a tangent screen (114 cm from the eye) with a hand-held projector or an automated projector system. In addition, bipolar stimulating electrodes were placed in the optic chiasm to activate the ganglion cell axons antidromically. Each ganglion cell that was encountered was classified as X, Y, or W on the basis of responses to a large battery of tests. The tests included receptive field center size, cutoff velocity, linearity of spatial summation, and response latency to stimulation of the optic chiasm (*8, 10*). Additional properties that aided in the classification of W-cells were the presence of a characteristically sluggish response to visual stimulation and unusual (nonconcentric) receptive field organization (*8, 10, 11*).

The responses of ganglion cells in each group of cats to two of the tests are summarized in Figs. 1 and 2. Figure 1 shows the distribution of response latencies to electrical stimulation of the optic chiasm. The distribution was trimodal in normal cats, and most neurons classified as X-cells had latencies in the second mode, between 2 and 4 msec. That is, X-cells had conduction velocities intermediate between those of Y-cells and those of W-cells (in agreement with other studies) (*8*). After neonatal lesions, very few cells remained with latencies in the X-cell range. Adult lesions had a similar, but smaller, effect on the distribution of response latencies to optic chiasm stimulation.

Figure 2 shows the distribution of re-

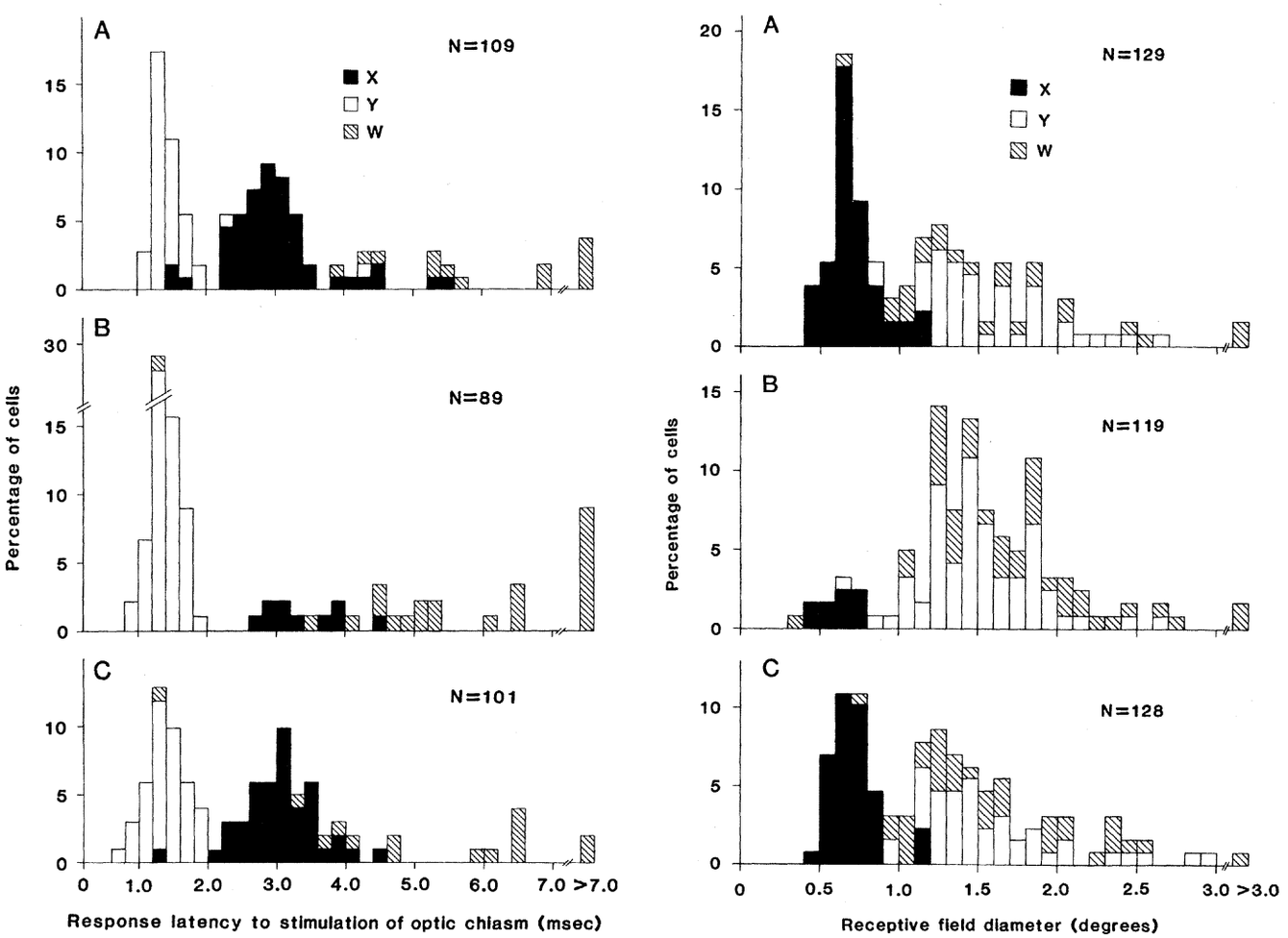

Fig. 1 (left). Frequency distributions of response latency to electrical stimulation of the optic chiasm for retinal ganglion cells in normal cats (A) and in cats with visual cortex lesions received on the day of birth (B) or as adults (C). Cells were classified as X, Y, or W on the basis of responses to a battery of tests. In the retinal area studied, Y-cells tended to have latencies ≤ 2 msec, X-cells from > 2 to ≤ 4 msec, and W-cells ≥ 3 msec. *N* indicates the number of cells tested. Fig. 2 (right). Frequency distributions of receptive field center diameter for retinal ganglion cells in normal cats (A) and in cats with visual cortex lesions received on the day of birth (B) or as adults (C). In the retinal area studied, X-cells tended to have receptive field diameters < 1° and Y- and W-cells ≥ 1°.

ceptive field center diameters. In normal cats the distribution was bimodal and, in agreement with previous studies (*8*), neurons classified as X-cells tended to have the smallest receptive fields (< 1° of arc). In cats with neonatal lesions the proportion of cells with small receptive fields was markedly reduced (*12*). By contrast, there was only a slight reduction in these cells after adult lesions.

Results for cutoff velocity and linearity of spatial summation suggested similar conclusions to those reached from Figs. 1 and 2. In general, we found that all the tests led to the same classification of each cell. This agreement was found for cells in all three groups of cats. Thus the cortical lesions produced a loss of a class of cells with a constellation of correlated response properties rather than an alteration of only a few specific properties used to classify cells.

To quantify the effects of the lesions, we determined the percentage of cells classified as X, Y, or W in the retina of each cat and calculated the mean and standard error for each group (Fig. 3A). In normal cats, 46 percent of the retinal ganglion cells were X-cells (range, 31 to 57 percent). This was reduced to 10 percent (range, 0 to 23 percent) in cats with neonatal lesions and 36 percent (range, 33 to 42 percent) in cats with adult lesions. The proportions of Y- and W-cells increased correspondingly. Thus the cortical lesions produced a loss of X-cells relative to Y- and W-cells.

To determine whether the loss was specific to X-cells, we analyzed the absolute retinal sampling density for each type of ganglion cell (that is, the percentage of retinal penetrations in which each cell type was encountered). There were no significant differences among the three groups of cats in the sampling densities of Y- or W-cells (Fig. 3B). This was true for subtypes of W-cells as well (*8*). In contrast, the sampling density of X-cells was significantly lower than normal in both the neonatal ($P < .001$) (Mann-Whitney U test) and the adult lesion groups ($P = .009$). In addition, the sampling density of X-cells was significantly lower in animals with neonatal lesions than in animals with adult lesions ($P = .001$). Thus the effects of the cortical lesions were specific to X-cells.

At the end of the recordings, brains with cortical lesions were processed for histological analysis. The adult and neonatal lesions were similar to those illustrated by Spear *et al.* (*13*). For each cat, the pattern of retrograde degeneration in the dorsal lateral geniculate and medial interlaminar nuclei was analyzed to determine the regions of visual field representation that were removed in areas 17, 18, and 19 (*13*). All ganglion cells studied had retinal locations corresponding to regions removed in areas 17 and 18, and about 65 percent of the cells in both groups had corresponding regions removed in area 19 as well. For both adult and neonatal lesions, the effects of removing areas 17 and 18 were similar to those of removing areas 17, 18, and 19. Therefore, the loss of X-cells probably can be attributed to the removal of cortical areas 17 and 18 alone.

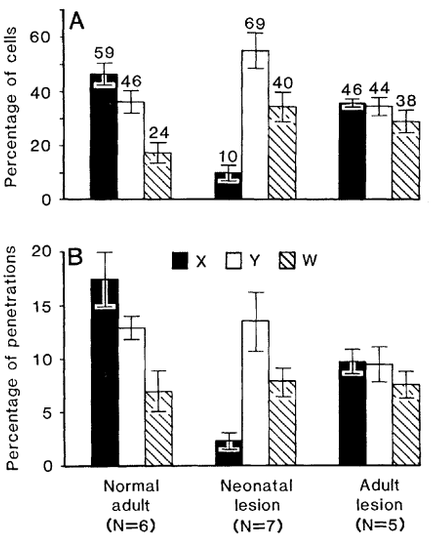

Fig. 3. (A) Percentage of retinal ganglion cells classified as X-, Y-, or W-cells in normal cats and in cats with visual cortex lesions received on the day of birth or as adults. *N* indicates the number of cats in each group. Bars show the means and brackets show the standard errors of the percentage of cells in each class for individual animals. The number above each bar gives the total number of cells in each class across animals. (B) Percentage of retinal penetrations in which X-, Y-, or W-cells were encountered in each group of cats.

We have shown that visual cortical lesions produce a transneuronal retrograde loss that is limited to a specific functional class of retinal ganglion cells, the X-cells. Relative encounter rates indicate that 78 percent of X-cells are lost after neonatal lesions of cortical areas 17 and 18. This figure agrees well with estimates of the medium-sized ganglion cell loss seen in anatomical studies of the cat retina (*5, 6*). In addition, we have shown that there is a smaller (22 percent) loss of X-cells following visual cortical lesions in adult cats.

The reason that X-cells are selectively affected by visual cortical lesions may be related to differences in axon branching patterns among the three classes of retinal ganglion cells (*7*). There is evidence that most or all retinal Y- and W-cells that project to the dorsal lateral geniculate nucleus (LGN) also send collateral projections to the midbrain, whereas approximately 90 percent of retinal X-cells project only to the LGN (*14*). Visual cortical lesions in both neonates and adults produce severe retrograde degeneration in the LGN, and the loss of their sole target neurons could in turn cause retinal X-cells to degenerate. In contrast, the remaining collateral branch of retinal Y- and W-cells to the midbrain appears sufficient to sustain their normal function (*15*).

It is not clear, however, why the loss of retinal X-cells is more severe after neonatal lesions than after adult lesions. It is known that neurons that fail to establish synaptic connections during development are rapidly eliminated (*16*). Since relatively few retinogeniculate synapses are present in the newborn kitten (*17*), the retrograde loss of LGN target neurons due to cortical removal at birth would be expected to produce a loss of retinal X-cells. However, it remains a mystery why mature retinal ganglion cells that have already formed connections are much more resistant to cell death in the LGN (*18*).

The greater loss of retinal ganglion cells after neonatal lesions presents a paradox when considered in light of other changes in the visual system. Previous anatomical and physiological studies in cats indicated that compensatory changes occur in the central visual pathways following visual cortical damage in neonates that do not occur following damage in adults (*13, 19*). Similarly, behavioral recovery can be more complete after neonatal damage than after adult damage (*1*). The present results indicate that this superior plasticity and compensation in the neonatal visual system occurs despite a much more severe loss of retinal X-cells than in adults. A resolution of this paradox may provide insights into why the infant brain responds to damage differently from the adult brain. In any case, this retinal abnormality needs to be considered when interpreting studies of behavioral deficits and neural mechanisms of recovery following visual cortex damage.

LILLIAN TONG
PETER D. SPEAR
Department of Psychology, University of Wisconsin, Madison 53706
RONALD E. KALIL
Department of Ophthalmology, University of Wisconsin
EILEEN C. CALLAHAN
Neurosciences Training Program, University of Wisconsin

References and Notes

1. P. D. Spear, *Prog. Psychobiol. Physiol. Psychol.* **8**, 45 (1979).
2. R. D. Lund, *Development and Plasticity of the Brain* (Oxford, New York, 1978).
3. J. M. Van Buren, *The Retinal Ganglion Cell Layer* (Thomas, Springfield, Ill., 1963); A. Cowey, *Perception* **3**, 257 (1974); R. E. Weller and J. H. Kaas, *Assoc. Res. Vision Ophthalmol. Abstr.* (1980), p. 2.
4. J. T. Dineen and A. E. Hendrickson, *Invest. Ophthalmol. Visual Sci.* **21**, 749 (1981).
5. R. E. Kalil, *Soc. Neurosci. Abstr.* **4**, 633 (1978); *ibid.* **6**, 790 (1980).
6. H. E. Pearson, D. R. Labar, B. R. Payne, P. Cornwell, N. Aggarwal, *Brain Res.* **212**, 470 (1981).
7. R. E. Weller, J. H. Kaas, A. B. Wetzel, *ibid.* **160**, 134 (1979).
8. Physiological studies have identified three functional classes of ganglion cells in the cat and monkey retina. These classes are termed X (or brisk sustained), Y (or brisk transient), and W (or sluggish). The cells are distinguished on the basis of their receptive field organization, dynamic response properties, and axonal conduction velocities. See R. W. Rodieck [*Annu. Rev. Neurosci.* **2**, 193 (1979)] for a review.
9. R. Otsuka and R. Hassler, *Arch. Psychiatr. Z. Gesamte Neurol.* **203**, 212 (1962).
10. Details of recording and sampling procedures are described by P. D. Spear, K. R. Jones, S. R. Zetlan, E. E. Geisert, and S. E. Kornguth [*J. Neurophysiol.* **47**, 1174 (1982)].
11. About half the W-cells had linear spatial summation and about half had nonlinear summation. Therefore, this property could not be used to distinguish W-cells from X- or Y-cells.
12. Recordings from surviving lateral geniculate neurons in cats whose visual cortex was removed at birth show that many of these cells develop abnormally large receptive fields [E. H. Murphy and R. E. Kalil, *Science* **206**, 713 (1979)]. It was originally proposed that these large receptive fields arise from a widespread convergence of retinal afferents onto surviving geniculate cells. The present results support this proposal, since no retinal ganglion cells with abnormally large receptive fields were found in cats given lesions as neonates.
13. P. D. Spear, R. E. Kalil, L. Tong, *J. Neurophysiol.* **43**, 851 (1980).
14. D. B. Bowling and C. R. Michael, *Nature (London)* **286**, 899 (1980); Y. Fukuda and J. Stone, *J. Neurophysiol.* **37**, 749 (1974); K.-P. Hoffmann, *ibid.* **36**, 409 (1973); R.-B. Illing and H. Wässle, *J. Comp. Neurol.* **202**, 265 (1981).
15. J. E. Rose and C. N. Woolsey, in *The Biological and Biochemical Bases of Behavior*, H. F. Harlow and C. N. Woolsey, Eds. (Univ. of Wisconsin Press, Madison, 1958), pp. 127–150.
16. W. M. Cowan, in *Development and Aging in the Nervous System*, M. Rockstein, Ed. (Academic Press, New York, 1973), pp. 19–41.
17. R. E. Kalil and G. Scott, *Soc. Neurosci. Abstr.* **5**, 791 (1979); D. A. Winfield and T. P. S. Powell, *Proc. R. Soc. London Ser. B* **210**, 197 (1980).
18. K. L. Chow and J. H. Dewson, *J. Comp. Neurol.* **128**, 63 (1966).
19. R. E. Kalil, L. Tong, P. D. Spear, *Assoc. Res. Vision Ophthalmol. Abstr.* (1979), p. 157; D. R. Labar, N. E. Berman, E. H. Murphy, *J. Comp. Neurol.* **197**, 639 (1981).

20. We thank K. Vielhuber and S. Miller for excellent technical assistance. Supported by Public Health Service postdoctoral fellowship EY05256 (L.T.), research grants EY01916, EY02545 (P.D.S.), and EY01331 (R.E.K.), and research career development award EY00089 (P.D.S.).

28 December 1981; revised 20 April 1982

Ontogeny of Gastric Acid Secretion in the Rat: Evidence for Multiple Response Systems

Abstract. *Gastric acid secretion has been thought to depend on histamine stimulation of the parietal cell. However, in the 2-week-old rat neither exogenous histamine nor the H-2 receptor agonist impromidine stimulates acid secretion, whereas pentagastrin and the cholinergic agent bethanechol are potent stimuli. At this age, the effect of pentagastrin on acid secretion is not blocked by the H-2 receptor antagonist cimetidine, nor is it potentiated by impromidine. These data suggest that, in the rat pup, the acid secretory response to pentagastrin and cholinergic agents occurs before the histamine-mediated system is functional and operates independently of the actions of histamine.*

The role of histamine in the regulation of H^+ ion secretion from the gastric parietal cell has been debated for more than 30 years. Early data suggested the hypothesis that histamine is the final common stimulator of H^+ secretion (*1*). Gastrin and cholinergic agonists, which also stimulate acid secretion, were thought to do so by releasing histamine. This view was later supported by the discovery of the histamine-2 (H-2) receptor antagonists burimamide, metiamide, and cimetidine (*2*). These antagonists not only inhibit histamine-stimulated acid secretion but also block the effects of gastrin and cholinergic agents on acid secretion (*3*). However, in the dog, atropine inhibits the secretory response to pentagastrin, 2-deoxyglucose, and liver extract but not to histamine (*4*), an observation that does not support the hypothesis of a common pathway involving histamine.

An alternative hypothesis is that histamine, cholinergic agents, and gastrin act directly on their own parietal cell surface receptors. Each may stimulate H^+ secretion independently and may also potentiate the effects of the others (*5, 6*).

Evidence for the independent action of gastrin, histamine, and cholinergic agents comes from in vitro studies of dispersed canine parietal cells (*5*). Gastrin, histamine, and carbamylcholine can each stimulate oxygen uptake by the parietal cell. H-2 receptor antagonists block only the effects of histamine, atropine blocks only the effects of carbamylcholine, and neither blocks the effects of gastrin on oxygen uptake. This isolated cell system also provides in vitro evidence that potentiating interactions occur between these agents.

However, to date it has not been established in vivo whether gastrin or cholinergic agents directly stimulate H^+ secretion independently of the actions of histamine. In studying the ontogeny of acid secretion in the rat, I found that the secretory response to pentagastrin and bethanechol develops before the response to histamine. Hence gastrin and cholinergic agents appear capable of direct stimulation of H^+ secretion in animals unresponsive to histamine.

Wistar-derived rats were studied under pentobarbital anesthesia. Output of H^+ was determined by continuous saline perfusion of the innervated gastric lumen (*7*); samples of the perfusate were collected every 10 minutes, and each sample was automatically titrated to *p*H 7.0 with 0.01*N* NaOH. Drugs were infused through a jugular cannula. Rectal temperature was maintained at 35.5° ± 0.5°C by external regulation.

Data were analyzed by analysis of variance or linear regression on an IBM 370/158. Both the analyses of variance and linear regressions were corrected for repeated measures at appropriate levels of the analysis.

In 14- to 16-day-old pups, infusion of pentagastrin or bethanechol produced a fourfold to fivefold increse in H^+ output over infusion of saline. By contrast, infusion of histamine diphosphate through a dose range of 2 to 12 mg/kg per hour did not significantly increase H^+ secretion (Table 1) (*8*).

Histamine affects both H-1 and H-2 receptors, although only H-2 receptors are found on parietal cells. To exclude the possibility that interaction with H-1 receptors (such as those on arterioles)

Table 1. Effects of three secretagogues on acid output in 2-week-old rat pups. Values (microequivalents per hour) are means ± standard errors.

Substance	Dose	*N*	Acid output	
			Basal	Stimulated
Histamine	8 mg/kg per hour	10	7.62 ± 1.94	10.06 ± 0.61*
Pentagastrin	120 μg/kg per hour	14	6.78 ± 0.81	23.0 ± 0.3†
Bethanechol	1 mg/kg per hour	8	5.14 ± 0.7	27.1 ± 4.58†

*$P > .10$ (analysis of variance) (*8*). †$P < .01$.

0036-8075/82/0702-0075$01.00/0